International Journal of Energy Optimization and Engineering
Volume 11 • Issue 2

Prediction of Photovoltaic Panels Output Performance Using Artificial Neural Network

Abdelouadoud Loukriz, LMSE Laboratory, Biskra University, Algeria*
https://orcid.org/0000-0001-6558-5933
Djamel Saigaa, M'sila University, Algeria
Abdelhammid Kherbachi, Renewable Energy Development Center, Algeria
Mustapha Koriker, M'sila University, Algeria
Ahmed Bendib, Blida 1 University, Algeria
Mahmoud Drif, M'sila University, Algeria

ABSTRACT

To ensure the safe and stable operation of solar photovoltaic system-based power systems, it is essential to predict the PV module output performance under varying operating conditions. In this paper, the interest is to develop an accurate model of a PV module in order to predict its electrical characteristics. For this purpose, an artificial neural network (ANN) based on the backpropagation algorithm is proposed for the performance prediction of a photovoltaic module. In this modeling approach, the temperature and illumination are taken as inputs and the current of the mathematical model as output for the learning of the ANN-PV-Panel. Simulation results showing the performance of the ANN model in obtaining the electrical properties of the chosen PV panel, including I–V curves and P–V curves, in comparison with the mathematical model performance are presented and discussed. The given results show that the error of the maximum power is very small while the current error is about 10-8, which means that the obtained model is able to predict accurately the outputs of the PV panel.

KEYWORDS

Artificial Neural Network (ANN), Backpropagation Algorithm, Learning, Modeling, PV

INTRODUCTION

Today, energy is at the heart of the economy for all countries as well as the basis for all human activity. Over the years, energy resources have diversified in order to meet ever-increasing needs. The developed countries have moved from wood to coal, to hydrocarbons, to hydroelectricity, and finally to nuclear power. However, the use of fossil fuels is responsible for acid rain and global warming (IEA, 2019). On the other hand, the exploitation of nuclear energy presents risks of serious accidents, in addition to those induced by the management of the resulting waste, which can be radioactively dangerous for

DOI: 10.4018/IJEOE.309417 *Corresponding Author

several thousand years (Compaan, 2006),(Panchenko, 2021). Numerous countries have committed themselves under the Kyoto protocol to minimize their greenhouse gas emissions by 8% (Luther, 2005). Renewable energy such as wind, solar, hydropower and biomass have an important role to play in achieving this goal. More particularly, the solar energy resource starts to have a significant contribution to global energy production due to the low cost of maintenance and recurring operation of the photovoltaic systems (Luther, 2005) (Antonanzas et al., 2016).

In the photovoltaic field, the manufacturers provide notations for PV modules under various metrological conditions. However, these conditions are not always evident, which rarely occur in outdoor conditions, as they are mostly performed under laboratory conditions using solar simulators (Naeijian et al., 2021). To this end, the accurate and efficient modeling of solar photovoltaic modules represents one of the most important and difficult problems in the field of photovoltaic systems. These problems are mainly caused by the non-linear characteristics of solar cells, and by the lack of availability of all their parameters (Cortés et al., 2020). Several mathematical models have been developed to characterize the PV module under different working conditions; the widely used being the diode-based model. The most well-known models in the literature are single diode and double diode. The model of the single diode is the simplest model that introduces 5 unknown parameters (Chegaar et al., 2001)(Cardenas et al., 2017)(Villalva et al., 2009), while the double diode model takes into account more features than the double diode model with 7 unknown parameters (Chan & Phang, 1987)(Mathew et al., 2018)(Ishaque et al., 2011). However, the main problem that should be dealt with is the estimation of the unknown parameters of the PV panel model.

To estimate the parameters of a PV panel, various methods have been suggested in the literature. In general, there are two categories of methods: deterministic as well as heuristic methods. In deterministic terms, the methods are classified into analytical and iterative approaches (Waly et al., 2019). The analytical techniques use information from the PV datasheet to estimate the parameters. Among the analytical methods, reduced space search (RSS) (Cardenas et al., 2017), Lambert-W based methods (Peñaranda Chenche et al., 2018), and OSMP based methods (Tong & Pora, 2016). The above-outlined approaches are complex and time-consuming because they solve the non-linear equations to determine the unknown parameters of the PV cell model. The second approach of deterministic methods is that of iterative ones, where the parameters are derived via trial and error and/or iteration. Among them, the Newton-Raphson method (Easwa Rakhanthan et al., 1986) (Ayang et al., 2019), Gauss-Seidel method (Chatterjee et al., 2011), and the Least-Squares (LS) technique (El Achouby et al., 2018). However, the application of iterative methods requires the system equations to be convex, continuous, and differentiable, which restricts the application of these methods. Furthermore, the selection of appropriate initial values in iterative methods is an important issue, in which a wrong choice can lead to getting stuck in local optima (Qais et al., 2020). To overcome the above-mentioned drawbacks of deterministic methods, scientists have oriented themselves towards heuristic methods; the unknown parameters of the PV model being determined by solving an optimization problem. The problem of parameter estimation in heuristic methods is treated as a black-box problem, in this case, it is not necessary to apply certain restrictions to the system equations, in contrast to deterministic methods (Naeijian et al., 2021). According to the literature, a variety of heuristic methods have been successfully applied to extract the PV parameters, among them; Particle Swarm Optimization (PSO) (Ye et al., 2009), Simulated Annealing (SA) (El-Naggar et al., 2012), Artificial Bee Colony Algorithm (ABC) (Oliva et al., 2014), Genetic Algorithm (GA) (Ismail et al., 2013), Salp Swarming Algorithm (SSA) (Abbassi et al., 2019), Enriched HHO (EHHO) (Chen et al., 2020), and Springy whale optimization algorithm (SWOA) (Pourmousa et al., 2021).

Despite heuristic methods showing better accuracy and performance than deterministic methods, some heuristic methods require a significantly high number of iterations to converge, where different results are found by repeating the function.

The Artificial Intelligence (AI) has been used for solving complicated problems in several application areas, including pattern recognition, identification, classification, speech, vision,

prediction, and control systems (Vasant et al., 2019), (Vasant et al., 2021a), (Vasant et al., 2021b), (Ganesan et al., 2020). Recently, artificial neural networks (ANNs) have been used to model the PV modules for obtaining the electrical characteristics (*I-V* or *P-V* curves). For instance, the authors (Hadjab et al., 2012) and (Mekki et al., 2007) have been utilized the ANN to estimate the behavior of the PV module, where the input/output data for learning the network are obtained in simulation by an adequate mathematical model.

This study presents the neural modeling of the PV array only for certain values of standard metrological conditions (i.e., temperature; T=25°C; and illumination; G=1000W/m^2). But, for inputs with arbitrary values, the results found have uncertainties with respect to the desired results obtained by the mathematical model.

Based on the research works discussed above, we are interested in this paper on providing an accurate prediction of a PV output performance based on an artificial neural network. The work carried out in the scope of this paper gives rise to the following contributions:

- The first issue that we want to work on is the development of a multi-layered perception (MLP) neural network with two hidden layers. This ANN is optimized regarding the number of hidden neurons based on the trial-and-error technique.
- In order to ensure a good validation of the proposed ANN model for any input values, a simulation study is proposed. In this simulation study, a random choice (i.e., use of uniformly distributed random variables, "rand") of the inputs (atmospheric conditions) and the output voltage of the PV panel is considered for the training of the ANN model. The role of this choice is to cover the maximum possible combinations of temperature, illumination, and panel voltage.
- For the "off-line" adaptation of the weights of the ANN network, we use in our research work an algorithm of training, which is the backpropagation algorithm.

The rest of this paper is arranged as follows. In section 2, the mathematical modeling of the PV cell and the description of the chosen PV module are given. Next, an overview of the artificial neural network is provided in section 3. Section 4 describes in detail the proposed ANN modeling approach. The simulation results and discussions are highlighted in section 5. In section 6, the main conclusions of the present research work are reported.

PHOTOVOLTAIC SYSTEM

In this section, the modeling of a PV module and the description of the chosen module (BP-SX150S) are presented.

Modeling of a PV Panel

The equivalent circuit of a PV cell is presented in Fig. 1, in which the simplest single-diode model of a PV panel can be represented by a photo-generated current source (I_{ph}) in antiparallel with a diode, defined by the single-exponential Shockley equation (Naeijian et al., 2021), and the non-ideals are represented by the insertion of the resistance R_s (series resistance). The I_{pv}–V_{pv} characteristic of the solar cell is described by a nonlinear equation given as follows (Chegaar et al., 2001), (Cardenas et al., 2017):

$$I_{pv} = I_{ph} - I_s \left(e^{\frac{q\left(V_{pv} + R_S \cdot I_{pv}\right)}{\eta k T}} - 1 \right) \tag{1}$$

where V_{pv} represents the output voltage of one PV panel, I_s is the saturation current of the PV diode, q is the electrical charge ($q = 1.6 \times 10{-}19$ C), η is the p-n junction quality factor, k is the Boltzmann

Figure 1. Equivalent circuit of the solar cell (single-diode three-parameters model)

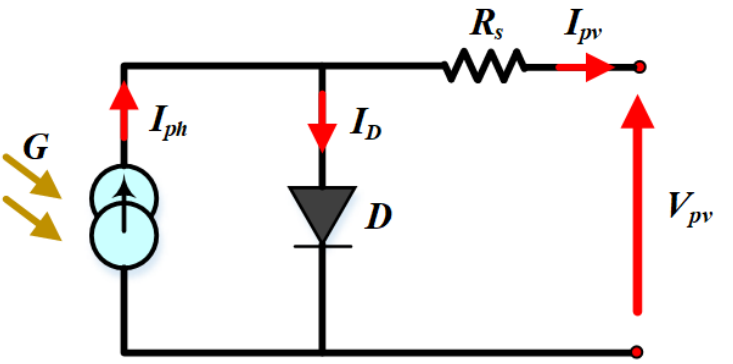

constant ($k = 1.38 \times 10{-}23$ J/K), T is the ambient temperature (in kelvins), and I_{ph} is the generated photocurrent related to the solar irradiation as described in the following equation:

$$I_{ph} = \left[I_{sc} + k_i\left(T - T_r\right)\right] \cdot \frac{G}{1000} \tag{2}$$

being I_{sc} the cell short-circuit current at adequate temperature; T_r the cell reference temperature, k_i the short-circuit current temperature coefficient, and G the solar illumination in W/m^2.

Equation (1) can be modified in order to present a null root when the current I_{pv} approaches the real PV current. So, (1) can be defined by (3) as a function of its PV current as follows:

$$f\left(I_{pv}\right) = I_{ph} - I_{pv} - I_s\left(e^{\frac{q\left(V_{pv}+R_S \cdot I_{pv}\right)}{\eta kT}} - 1\right) \tag{3}$$

The current I_{pv}, with a null initial value, is utilized in an iterative process that approximates (2) of its root, being obtained by the Newton–Raphson method (4), which seeks the zero of the differentiable equation:

$$X\left(n+1\right) = X\left(n\right) - \frac{f\left[X\left(n\right)\right]}{f'\left[X\left(n\right)\right]} \tag{4}$$

Therefore, the current I_{pv} can be calculated by (Easwarakhanthan et al., 1986):

$$I_{pv}\left(n+1\right) = I_{pv}\left(n\right) - \frac{I_{ph} - I_{pv}\left(n\right) - I_s\left(e^{\frac{\left(V_{pv}+R_S \cdot I_{pv}\left(n\right)\right)}{V_T}} - 1\right)}{-1 - I_s\left(e^{\frac{\left(V_{pv}+R_S \cdot I_{pv}\left(n\right)\right)}{V_T}} - 1\right)\left(\frac{R_S}{V_T}\right)} \tag{5}$$

where:

$$V_T = \frac{\eta k T}{q}$$

BP-SX150S Panel

In our study, we chose the BP-SX150S photovoltaic panel, due to its higher efficiency, compared to other panels from different manufacturers, hence, its maximum voltage is higher. In addition, it provides efficient power for general use by the direct operation of direct current (DC) loads, or alternating current (AC) loads on systems equipped with inverters. The panel consists of 72 polycrystalline silicon cells connected in series to produce 150W of power (Hornsberg & Bowden, 2018).

Manufacturers of solar panels specify the performance of their equipment under the following standard conditions (S.T.C):

- An AM 1.5 spectrum
- An illuminance of 1000W/m^2
- An ambient temperature of 25°

Based on the technical data sheets provided by the manufacturer, the parameters of the chosen panel are determined, and they are reported in Table 1.

Overview of ANN

Biological neural networks easily perform many applications such as pattern recognition, signal processing, learning (memorization and generalization). These applications are, however, despite all the efforts made in algorithmic and artificial intelligence, at the limit of the current possibilities. It is on the assumption that intelligent behavior emerges from the structure and behavior of the basic elements of the brain that artificial neural network. Artificial neural networks are models, as such; they can be described by their components, their descriptive variables, and the interactions of the components (Yegnanarayana, 1994), (Popoola et al., 2019).

Each artificial neuron is an elementary processor; it receives a variable number of inputs from upstream neurons. A weight (Wij) is associated with each of these inputs. Each elementary processor has a single output, which then branches to feed a variable number of downstream neurons. Each connection is associated with a synaptic weight (see Figure 2), this elementary structure is called perceptron (HARMON, 1959).

Table 1. BP-SX150S panel specifications at S. T. C

Parameter	Symbol	Value	Unit
Nominal Power	P_{nom}	150	W
Voltage at maximum power	V_{pm}	34.5	V
Current at maximum power	I_{pm}	4.35	A
Open circuit voltage	V_{oc}	43.5	V
Short-circuit current	I_{sc}	4.75	A
Temperature coefficient	a	0.065±0.015	mA/°C

Figure 2. A model of an artificial neuron network

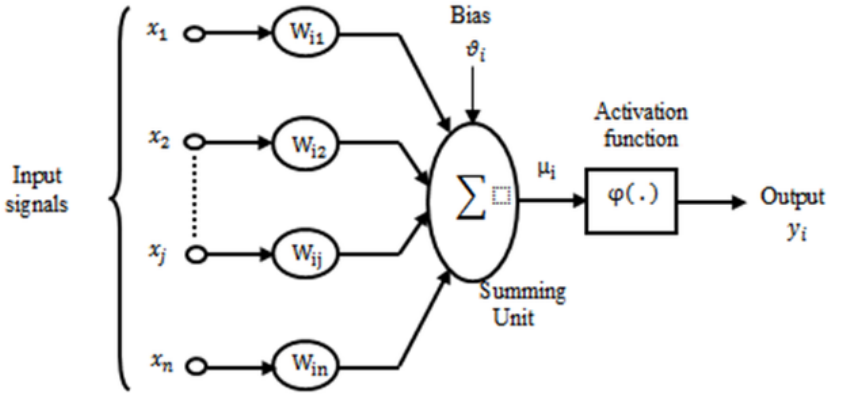

PROPOSED ANN MODELING APPROACH

In the photovoltaic field, manufacturers provide datasheets for PV modules at different meteorological conditions. However, these conditions are not always obvious, rarely occurring outdoors, as they are mainly carried out under laboratory conditions using a solar simulator. Therefore, in order to perform an appropriate characterization of the electrical behavior of PV panels (obtaining the I-V and P-V curves). The present research work focuses on developing a model based on artificial neural network to substitute it for the response of the BP-SX150S photovoltaic panel under different meteorological conditions.

The proposed multi-layer feed-forward neural network architecture for the modeling of the PV module is portrayed in figure 3. This architecture considers three inputs; cell temperature (T), solar illumination (G), and the output voltage of the PV module (V_{pv}); and one output which is the PV output current (I_{pv}). In addition, it consists of two hidden layers, in which the first hidden layer composes of 06 neurons and the second hidden layer of 10 neurons. The number of neurons in each hidden layer is chosen in optimum way considering the least MSE between the estimated current (I_{pv}) by the proposed ANN model and the one calculated using the PV mathematical equation. This process is done based on a simulation study in MATLAB/Simulink environment. The different obtained results are reported in Table 2, where the error converges to the minimum in architecture number 1, which justifies our choice.

It is worth noting that, the global database is divided into two bases, the learning base, and the test base. The learning base with the backpropagation algorithm is used to train the neural network, while the test base is exploited to check the performance of the obtained model. The database must cover this set of values. Based on the values of the different parameters, the database will therefore have 512×512×512 elements, and the training of the neural network is done with a database of 134217728 elements. It is important to notice that no part of the test base is used throughout the learning process. This database is reserved only for the final measurement of performance. In other words, to check whether the neural network performs well in the cases it has not learned "test basis".

To obtain the expected ANN-PV model, the procedure of the ANN is done based on the following phases:

1. **Normalization phase:** All the parameters used for the ANN modeling of the chosen PV panel (BP-SX150S) are summarized, hereafter:
   a. **Architecture:** Multi-layer perceptron (Feed-forward MLP)

Figure 3. Schematic diagram of the proposed neural network architecture

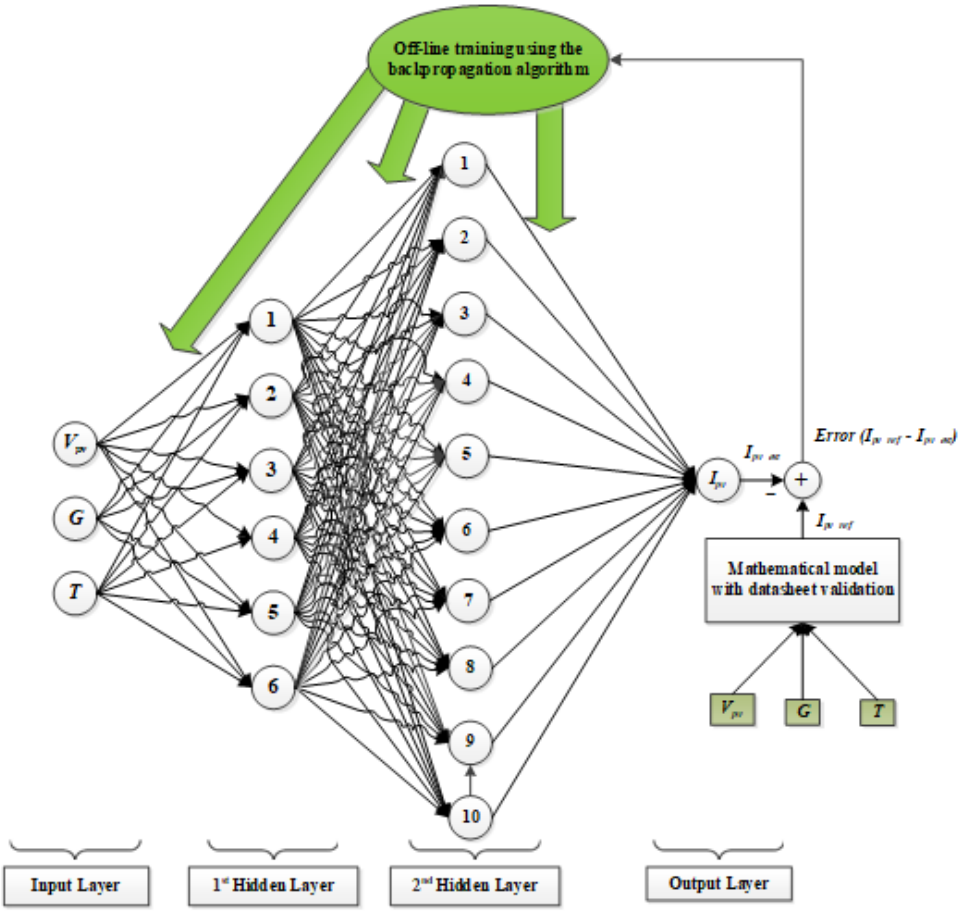

b. **Learning rule:** Backpropagation of errors
c. **Number of hidden layers:** 2
d. **Number of neurons in the input layer:** 3 (V_{pv}, G, T)
e. **The number of neurons in each hidden layer:** See below:
   i. **1st hidden layer:** 06 neurons
   ii. **2nd hidden layer:** 10 neurons
f. **The number of neurons in the output layer:** 1 (I_{pv})
g. **The functions:** See below:
   i. **1st hidden layer:** Sigmoid
   ii. **2nd hidden layer:** Sigmoid
h. **Input and output terminals:** See below:

Inputs: V_{pv} (V): min = 0V, max = 50V
G (W/m^2): min = 0W/m^2, max = 1000W/m^2
T (°C): min = 0°C, max = 100°C
Output: I_{pv} (A): min = 0A, max = 6A

Table 2. Variation of the test error according to the different structures

N	Number of neurons 1st hidden layer	Number of neurons 2nd hidden layer	MSE
1	6	10	0.00000113
2	7	4	0.0000225
3	7	5	0.0000553
4	7	9	0.00006614
5	6	5	0.000109
6	6	9	0.000202
7	5	10	0.000213
8	8	5	0.000324
9	6	8	0.000413
10	4	9	0.000464
11	5	8	0.000507
12	6	4	0.000722
13	4	7	0.00224
14	4	8	0.00225
15	5	4	0.00231
16	4	5	0.00285
17	5	5	0.00297
18	4	6	0.00357
19	5	9	0.00511
20	7	8	0.00622
21	6	7	0.00764
22	8	6	0.00768
23	7	6	0.0087
24	4	10	0.0156
25	5	6	0.0174
26	6	6	0.041
27	5	7	0.0634
28	7	7	0.08885
29	8	4	0.09476
30	7	10	0.099423

i. **Database:** See below:
   i. **Learning base:** 134217728
   ii. **Validation and test basis:** 40265318

j. **The error:** Desired error, E_d: 10^{-8}:
   i. **MSE:** 1.13×10^{-6}

2. **Learning phase:** Learning is a phase in the development of a neural network, in which the behavior of the network is modified until the desired behavior is achieved. After several executions of the program, the values of the learning coefficient ($\mu = 0.0002$) and the inertia (momentum) ($\alpha = 0.8$) are selected which gives the desired error with a fixed number of iterations. Figure 4 shows the flowchart that represents the implemented

Figure 4. Flow shat of the learning phase algorithm

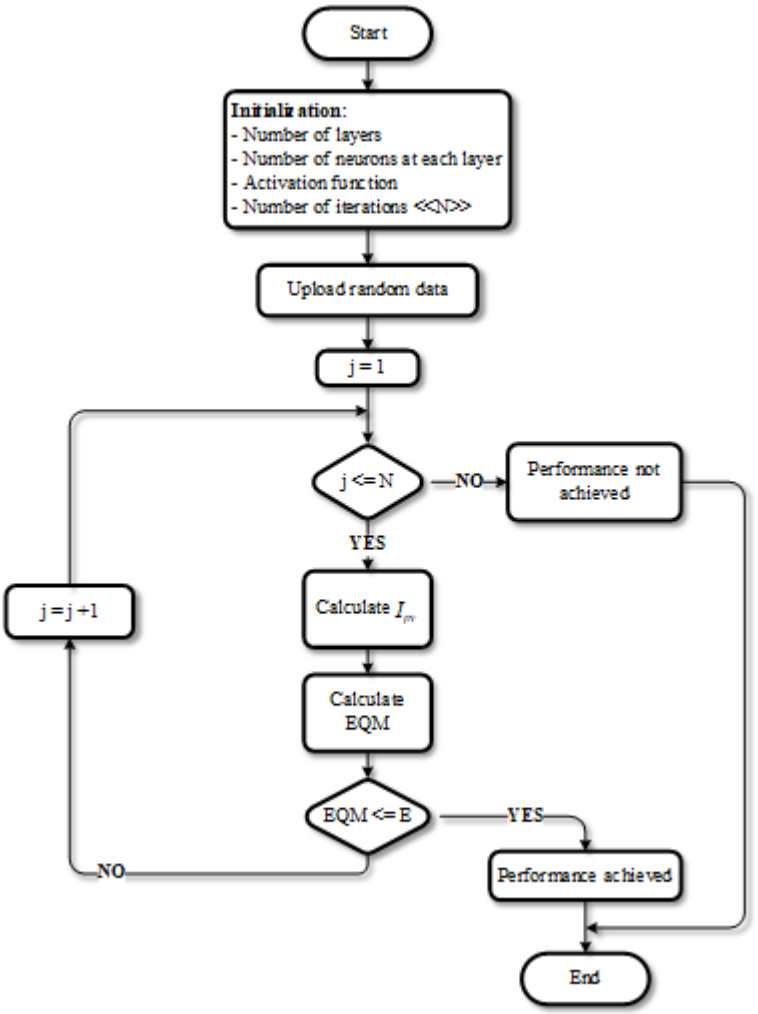

algorithm in MATLAB for the ANN training. Since, in our case, the number of neurons in the output layer is set by the number of system outputs to be modeled, the PV panel has a single output I_{pv} (output current). In figure 5, we present the detailed flowchart for learning the ANN model.

3. **Validation and test phase:** The evaluation of the generalization capacity of the neuronal system is carried out on a validation basis. Using input-output pairs that do not belong to the learning base. Indeed, after carrying out the learning and finding the network weights necessary for the calculation of the properties, the error must be estimated on a test basis. It is sufficient to compare the initial database with the one obtained after the training and to draw the current (power) curve modulating I_{pv} ($P_{pv} = I_{pv} \times V_{pv}$) for different values of V_{pv}, G, and T. The block diagram of the adopted algorithm for the ANN model validation is depicted in Figure 6.

Figure 5. Detailed flowchart for the learning task

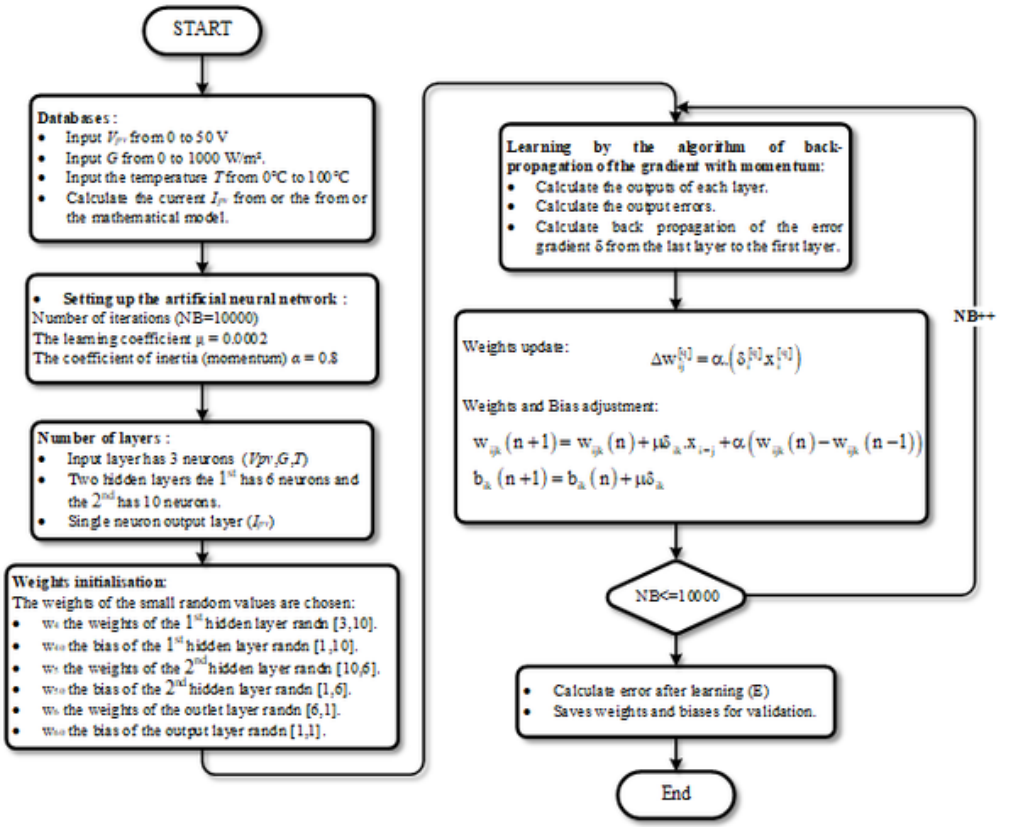

SIMULATION RESULTS AND DISCUSSIONS

In this section, the test-bed built to assess the obtained ANN model (given in figure 3) is shown in figure 7. In addition, the obtained results that show the performance of the obtained ANN model, in which the *I-V* and *P-V* characteristics, as well as the calculated relative error between the ANN model and the mathematical actual model, are provided. It's worth mentioning that the parameters used in this simulation study are the same given in the initialization phase.

I-V and PV Curves

Simulations in MATLAB are carried out to assess the performance of the obtained ANN model. Indeed, the comparison between the initial database and the one obtained after the learning phase, using the test base, has indicated that the proposed neural model faithfully expresses the variation in the response of the PV panel characterized.

Figures 8 and 9 show the performance of the ANN model obtained for different values of G with T = 25°C. In this test, the following four values of G are considered: 300 W/ m^2, 500 W/ m^2, 800 W/ m^2, 1000 W/m2. From these figures, it can be noticed that the I–V and P–V curves predicted with the proposed ANN model are matched with the ones given by the mathematical model for different values of irradiance G.

Figure 6. Validation flowchart

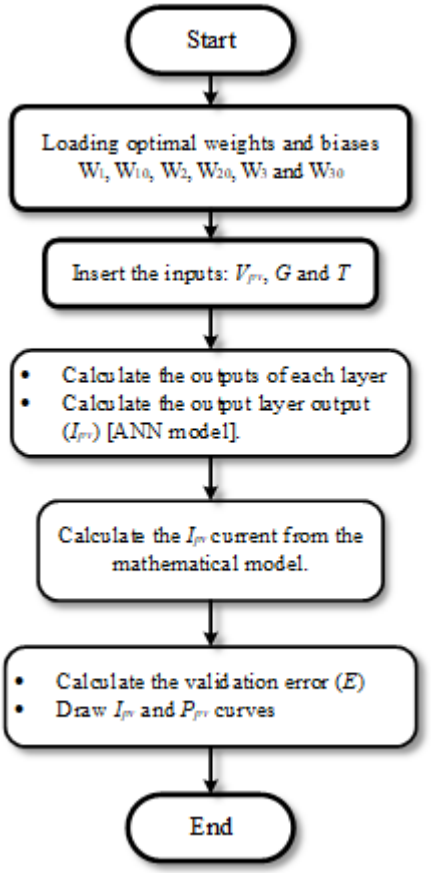

Figure 7. Block diagram of the built test-bed for assessing the performance of the ANN-panel model

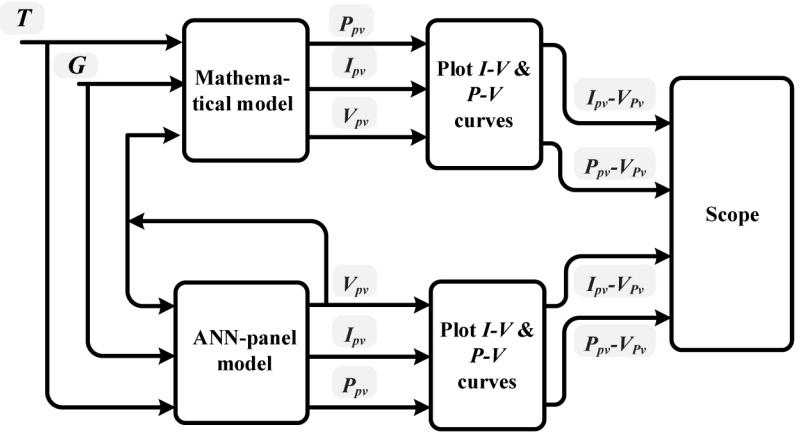

Figure 8. Current-voltage curve (mathematical model with ANN model) for different illuminations values and T = 25°C

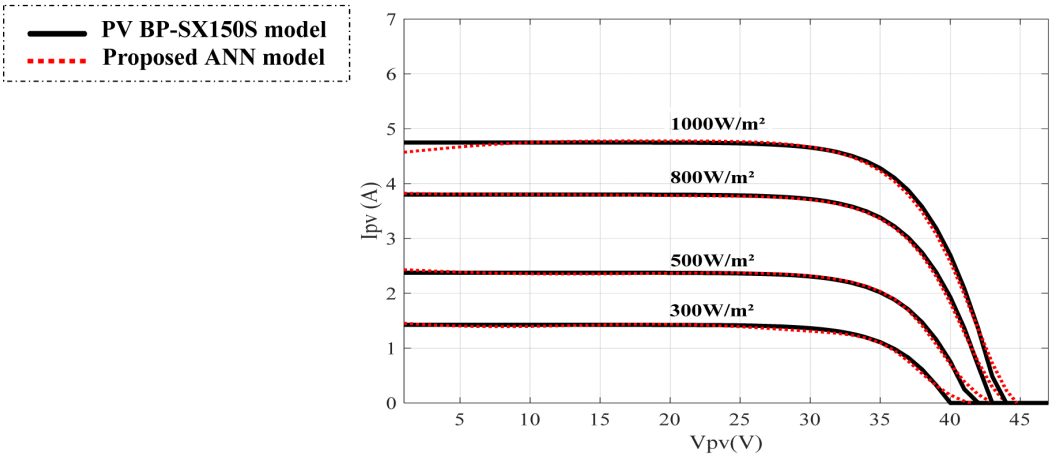

Figure 9. Power-voltage curve (mathematical model with ANN model) for different illumination G values and T = 25°C

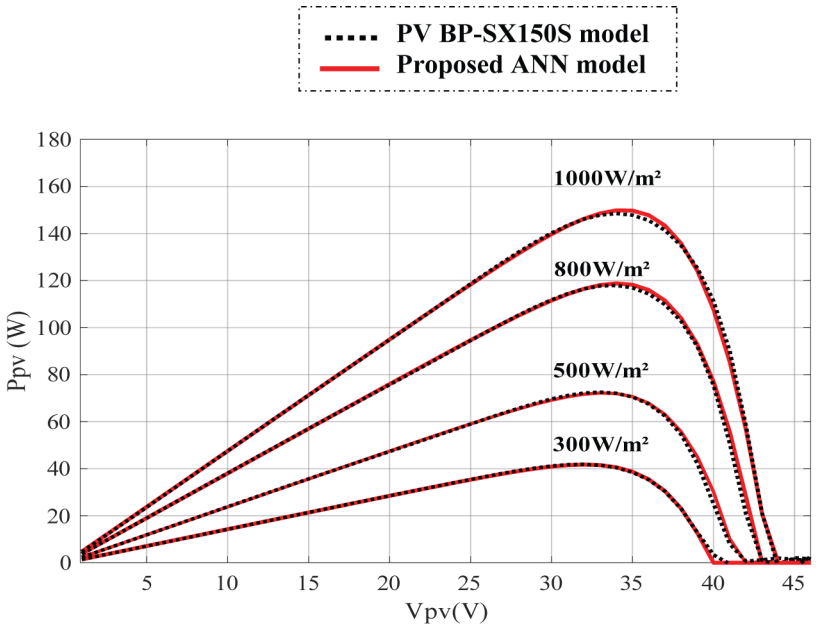

With the same procedures, we assess the performance of the proposed neural model carried out for different values of the temperature *T*. We took four values of temperature *T*, which are: 0 C°, 25 C°, 50 C°, and 75 C°. Figures 10 and 11 show the performance of the ANN model obtained for different values of *T* and $G = 1000\text{W/m}^2$. According to figures 10 and 11, it can be seen that the ANN model accurately predicts the I-V and P-V curves as the mathematical model for various values of the temperature *T*.

Figure 10. Current-voltage curve (mathematical model with ANN model) for different temperature T values and G = 1000W/m²

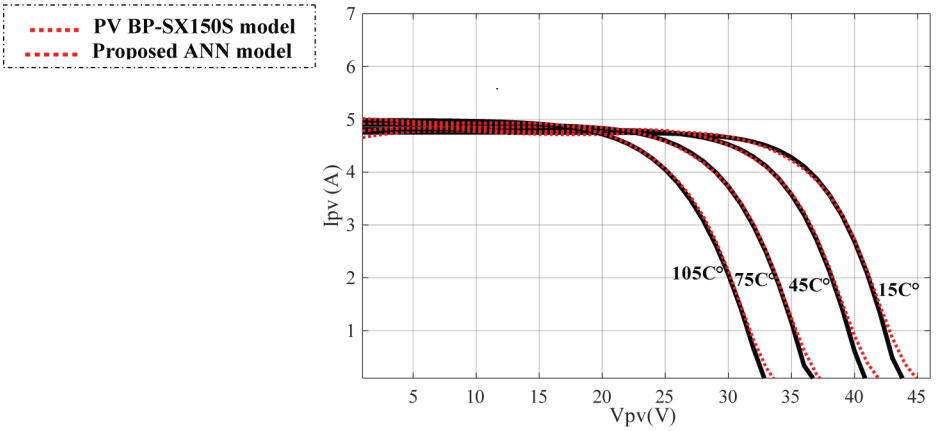

Figure 11. Power-voltage curve (mathematical model with ANN model) for different temperature values and G =1000W/m²

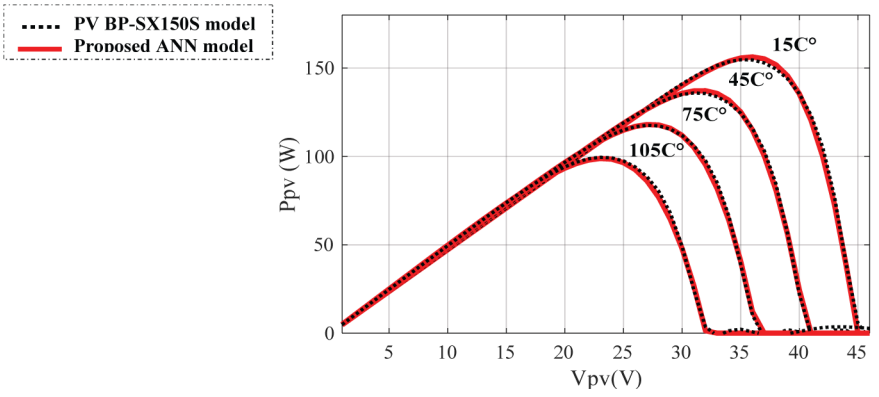

Error Calculation

To demonstrate further the effectiveness of the proposed ANN model, the relative error between the electrical PV parameters ; maximum power P_{pv_m}, open circuit voltage V_{OC} , and short circuit current $I_{SC;}$ predicted by the ANN model and the ones of the mathematical model is evaluated under several illumination and temperature conditions.

The relative error is defined as the difference between the values of the generated PV parameter by the two models; the mathematical model (Y_{pv}) and the obtained neural model ($\hat{Y}_{pv}$), divided by that of the mathematical model (Y_{pv}). This error is calculated using the expression given by equation (6) below:

$$E_r = \frac{\left|Y_{pv} - \hat{Y}_{pv}\right|}{Y_{pv}} \times 100\% \tag{6}$$

Maximum Power (P_{pv_m}) Error

Figure 12 depicts the relative error in P_{pv_m} of the BP-SX150S module at different irradiation levels, while the temperature is set at the STC condition ($T = 25°C$).

It can be observed that the relative error of the maximum power increases when the irradiance decreases. More particularly, in the case of high irradiation, i.e., in the value of 1000W/m², the relative error is around 0.02%, due to the good learning of the proposed model in STC conditions. Whereas, in the case of low values of irradiation, the maximum relative error does not exceed the value of 3.7%.

For temperature variation, Figure 13 shows the relative error in P_{pv_m} for the BP-SX150S module under different temperature values, and the irradiance is set to 1000 W/m² (STC condition). It is

Figure 12. Relative error of the maximum power for different values of G with T = 25°C

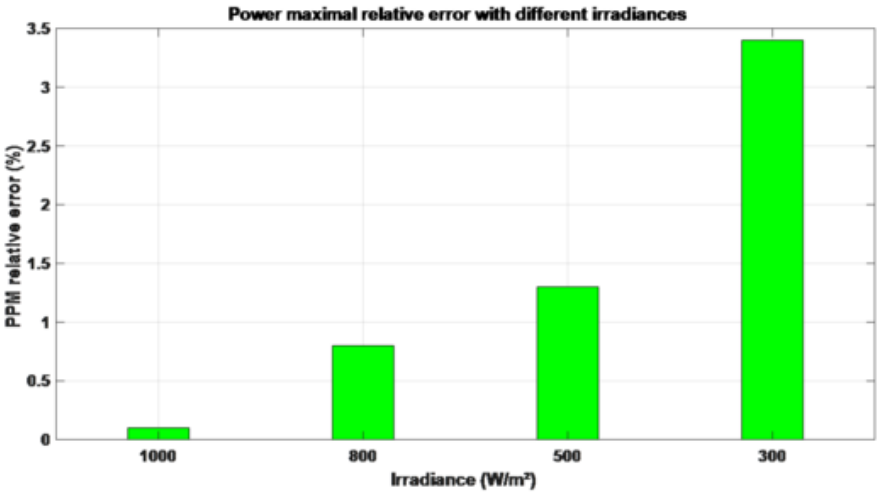

Figure 13. Relative error of the maximum power under different values of T with G = 1000 W/m²

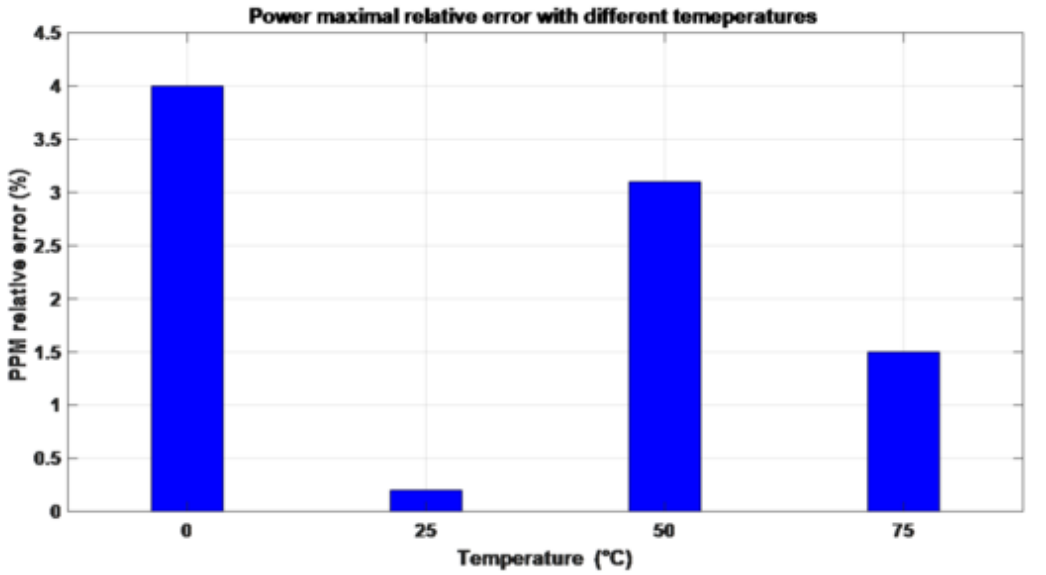

noticeable that the relative error of the maximum power for zero-temperature is important (4%) compared to other temperature values because the zero-temperature value is at the limit of the database space chosen for the training phase. However, the relative error of the maximum power for different temperature values does not exceed the value of 3.2%.

Open Circuit Voltage V_{OC} Error

Figure 14 shows the analytical relative error in V_{OC} for the BP-SX150S module under different illumination levels when the temperature value is set at 25 °C (STC condition). According to this figure, the relative error of the open-circuit voltage for different illuminance values is minimal, especially for 800 W/m^2 irradiance, which is of the order of $10^{-2\%}$.

The relative analytical error in V_{oc} for the BP-SX150S modules for different temperature values is shown in Figure 15 while the irradiance value was set in the STC condition. From this figure, it

Figure 14. Relative error of the open-circuit voltage Voc for different values of G with T = 25°C

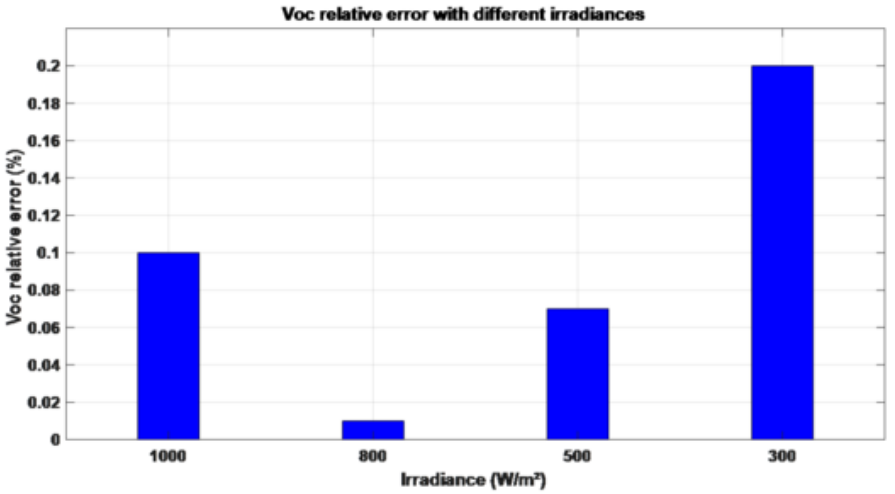

Figure 15. Relative error of the open-circuit voltage V_{oc} under different values of T with G = 1000 W/m²

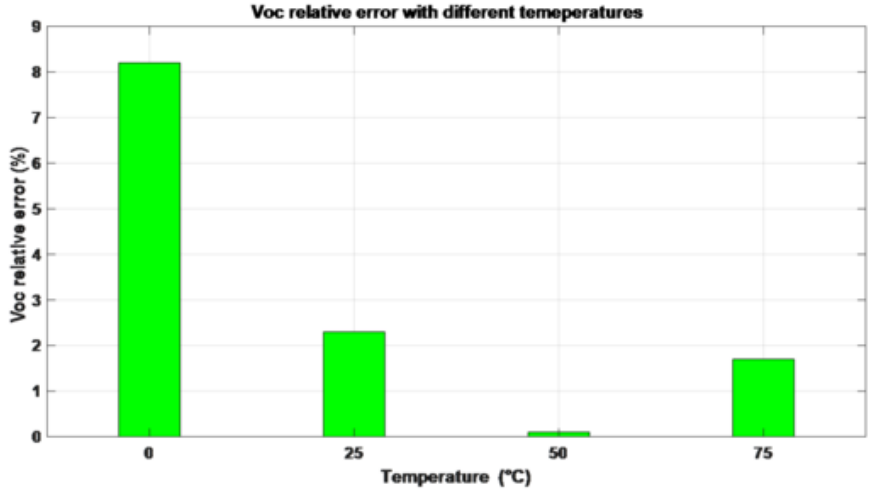

can be noted that the relative error is very small for the different values of temperature except the value 0°C, in which an error of about 8% is noticed.

Short-Circuit Current I_{sc} Error

Here, the performance of the proposed model for predicting the short circuit current I_{SC} under varying illumination and temperature conditions is assessed. Figures 16 and 17 show the relative error in I_{SC} for the BP-SX150S module at different illumination and temperature levels respectively. In the case of illumination variation, the maximum error value is 0.5% for the illumination value of 300 W/m^2, while the minimum value is 0.01% for the illumination value of 800 W/m^2. However, the maximum error value in the case of temperature variation is 0.75% for the temperature value of 25°C, whereas a minimum value of 0.1% is found when the temperature value is 50 °C.

Figure 16. Relative error of the short-circuit current I_{sc} under different values of G with T = 25°C

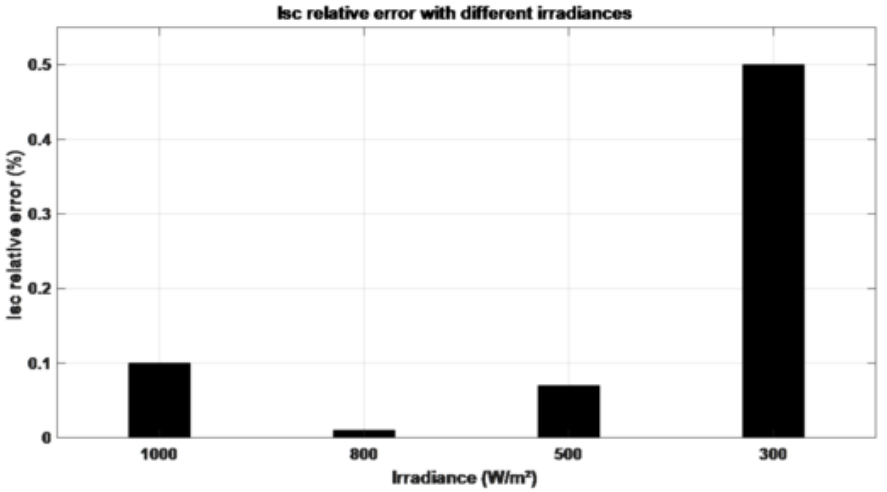

Figure 17. Relative error of the short circuit current I_{sc} for different values of T with G = 1000W/m^2

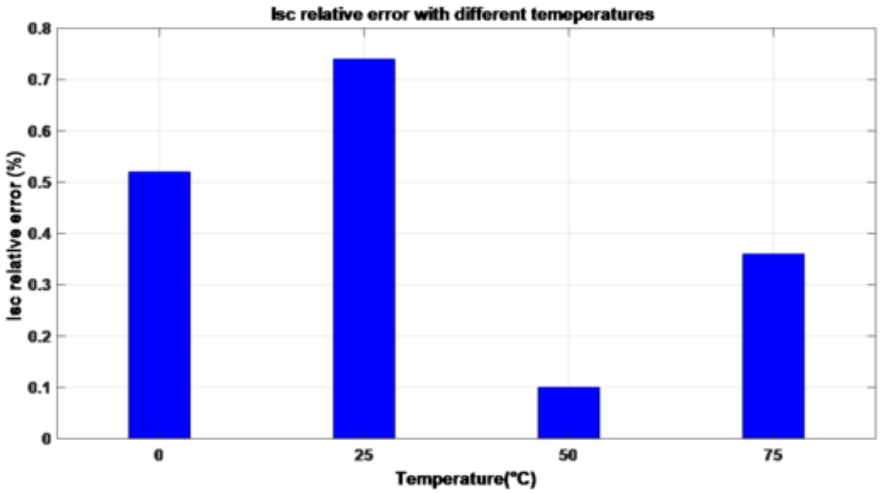

Generally speaking, it can be seen that the proposed neural model provides an accurate prediction for the shape of the I-V and P-V curves of the BP-SX150S photovoltaic module, compared with the mathematical model under different metrological conditions.

CONCLUSION

In this paper, a model of the BP-SX150S PV module based on a multi-layer feed-forward neural network trained with a back-propagation algorithm was developed. First, a good selection of the database is necessary where illumination range have been selected from 0 W/m^2 to 1000 W/m^2, and temperature range from 0 C° to 100C°. As far as the output voltage was concerned, a range of 0V to 50V has been set in the training phase. It is necessary to note that the training set is very important, it must represent a fairly large set of PV module behavior so that our artificial neural network is well trained. In addition, the neural network has been optimized in terms of number of hidden neurons by using the trial-and-error technique. An MSE in the output current was reached up to 10^{-8} in the training phase. Once all the training steps have been completed, the performance of the proposed neural model against the learning data has been evaluated, which is necessary to check its reliability. Second, the performance of the proposed neural model has been tested for inputs that were not confronted during the learning phase. The obtained results have shown that the proposed neural model can provide an accurate prediction for the shape of the curves of the supplied current versus the voltage and produced power versus the voltage. Also, they have presented that the calculated relative error between the maximum power produced by the ANN model and the mathematical model was reached up to 0.02%. Thus, the maximum power delivered by the ANN is very close to that obtained by the BP-SX150S model. This model can be very useful for academic researchers and engineers in applications where precise prediction of the outputs of a BP-SX150S module is needed. As perspectives, the extension of this research work can be envisaged, it is a way to apply a real database (experimental data of our city; M'sila, Algeria) for optimal neuronal modeling of the photovoltaic module.

REFERENCES

Abbassi, R., Abbassi, A., Heidari, A. A., & Mirjalili, S. (2019). An efficient salp swarm-inspired algorithm for parameters identification of photovoltaic cell models. *Energy Conversion and Management*, *179*, 362–372. doi:10.1016/j.enconman.2018.10.069

Alfa, A. A., Misra, S., Abayomi-Alli, A., Arogundade, O., Jonathan, O., & Ahuja, R. (2021). Comparative Analysis of Intelligent Solutions Searching Algorithms of Particle Swarm Optimization and Ant Colony Optimization for Artificial Neural Networks Target Dataset. In Lecture Notes in Networks and Systems (pp. 459–470). doi:10.1007/978-981-16-0733-2_32

Antonanzas, J., Osorio, N., Escobar, R., Urraca, R., Martinez-de-Pison, F. J., & Antonanzas-Torres, F. (2016). Review of photovoltaic power forecasting. Solar Energy. doi:10.1016/j.solener.2016.06.069

Ayang, A., Wamkeue, R., Ouhrouche, M., Djongyang, N., Essiane Salomé, N., Pombe, J. K., & Ekemb, G. (2019). Maximum likelihood parameters estimation of single-diode model of photovoltaic generator. *Renewable Energy*, *130*, 111–121. doi:10.1016/j.renene.2018.06.039

Cardenas, A. A., Carrasco, M., Mancilla-David, F., Street, A., & Cardenas, R. (2017). Experimental Parameter Extraction in the Single-Diode Photovoltaic Model via a Reduced-Space Search. *IEEE Transactions on Industrial Electronics*, *64*(2), 1468–1476. doi:10.1109/TIE.2016.2615590

Chan, D. S. H., & Phang, J. C. H. (1987). Analytical Methods for the Extraction of Solar-Cell Single-and Double-Diode Model Parameters from I-V Characteristics. *IEEE Transactions on Electron Devices*, *34*(2), 286–293. doi:10.1109/T-ED.1987.22920

Chatterjee, A., Keyhani, A., & Kapoor, D. (2011). Identification of Photovoltaic Source Models. *IEEE Transactions on Energy Conversion*, *26*(3), 883–889. doi:10.1109/TEC.2011.2159268

Chegaar, M., Ouennoughi, Z., & Hoffmann, A. (2001). New method for evaluating illuminated solar cell parameters. *Solid-State Electronics*, *45*(2), 293–296. doi:10.1016/S0038-1101(00)00277-X

Chen, H., Jiao, S., Wang, M., Heidari, A. A., & Zhao, X. (2020). Parameters identification of photovoltaic cells and modules using diversification-enriched Harris hawks optimization with chaotic drifts. *Journal of Cleaner Production*, *244*, 118778. doi:10.1016/j.jclepro.2019.118778

Compaan, A. D. (2006). Photovoltaics: Clean power for the 21st century. *Solar Energy Materials and Solar Cells*, *90*(15), 2170–2180. doi:10.1016/j.solmat.2006.02.017

Cortés, B., Tapia Sánchez, R., & Flores, J. J. (2020). Characterization of a polycrystalline photovoltaic cell using artificial neural networks. *Solar Energy*, *196*, 157–167. doi:10.1016/j.solener.2019.12.012

Easwarakhanthan, T., Bottin, J., Bouhouch, I., & Boutrit, C. (1986). Nonlinear Minimization Algorithm for Determining the Solar Cell Parameters with Microcomputers. *International Journal of Solar Energy*, *4*(1), 1–12. doi:10.1080/01425918608909835

El Achouby, H., Zaimi, M., Ibral, A., & Assaid, E. M. (2018). New analytical approach for modelling effects of temperature and irradiance on physical parameters of photovoltaic solar module. *Energy Conversion and Management*, *177*, 258–271. doi:10.1016/j.enconman.2018.09.054

El-Naggar, K. M., AlRashidi, M. R., AlHajri, M. F., & Al-Othman, A. K. (2012). Simulated Annealing algorithm for photovoltaic parameters identification. *Solar Energy*, *86*(1), 266–274. doi:10.1016/j.solener.2011.09.032

Hadjab, M., Berrah, S., & Abid, H. (2012). Neural network for modeling solar panel. *INTERNATIONAL JOURNAL OF ENERGY*, *6*(1), 9–16.

Harmon, L. D. (1959). Artificial Neuron. *Science*, *129*(3354), 962–963. doi:10.1126/science.129.3354.962 PMID:17817093

Hornsberg, C., & Bowden, S. (2018). *Silicon Solar Cell Parameters*. PV Education.

IEA. (2019). *Renewables 2019 – Analysis*. International Energy Agency.

Ishaque, K., Salam, Z., & Taheri, H. (2011). Simple, fast and accurate two-diode model for photovoltaic modules. *Solar Energy Materials and Solar Cells*, *95*(2), 586–594. doi:10.1016/j.solmat.2010.09.023

Ismail, M. S., Moghavvemi, M., & Mahlia, T. M. I. (2013). Characterization of PV panel and global optimization of its model parameters using genetic algorithm. *Energy Conversion and Management*, *73*, 10–25. doi:10.1016/j.enconman.2013.03.033

Luther, J. (2005). Motivation for Photovoltaic Application and Development. In *Handbook of Photovoltaic Science and Engineering* (pp. 45–60). John Wiley & Sons, Ltd. doi:10.1002/0470014008.ch2

Mathew, D., Rani, C., Rajesh Kumar, M., Wang, Y., Binns, R., & Busawon, K. (2018). Wind-Driven Optimization Technique for Estimation of Solar Photovoltaic Parameters. *IEEE Journal of Photovoltaics*, *8*(1), 248–256. doi:10.1109/JPHOTOV.2017.2769000

Mekki, H., Mellit, A., Salhi, H., & Khaled, B. (2007). Modeling and simulation of photovoltaic panel based on artificial neural networks and VHDL-language. *2007 14th IEEE International Conference on Electronics, Circuits and Systems*, 58–61. doi:10.1109/ICECS.2007.4510930

Messalti, S., Harrag, A. G., & Loukriz, A. E. (2015). A new neural networks MPPT controller for PV systems. *IREC2015 The Sixth International Renewable Energy Congress*, 1–6. doi:10.1109/IREC.2015.7110907

Naeijian, M., Rahimnejad, A., Ebrahimi, S. M., Pourmousa, N., & Gadsden, S. A. (2021). Parameter estimation of PV solar cells and modules using Whippy Harris Hawks Optimization Algorithm. *Energy Reports*, *7*, 4047–4063. doi:10.1016/j.egyr.2021.06.085

Oliva, D., Cuevas, E., & Pajares, G. (2014). Parameter identification of solar cells using artificial bee colony optimization. *Energy*, *72*, 93–102. doi:10.1016/j.energy.2014.05.011

Panchenko, V. (2021). Photovoltaic Thermal Module With Paraboloid Type Solar Concentrators. *International Journal of Energy Optimization and Engineering*, *10*(2), 1–23. doi:10.4018/IJEOE.2021040101

Peñaranda Chenche, L. E., Hernandez Mendoza, O. S., & Bandarra Filho, E. P. (2018). Comparison of four methods for parameter estimation of mono- and multi-junction photovoltaic devices using experimental data. *Renewable & Sustainable Energy Reviews*, *81*, 2823–2838. doi:10.1016/j.rser.2017.06.089

Popoola, S. I., Faruk, N., Oloyede, A. A., Atayero, A. A., Surajudeen-Bakinde, N. T., & Olawoyin, L. A. (2019). Characterization of Path Loss in the VHF Band using Neural Network Modeling Technique. *Proceedings - 2019 19th International Conference on Computational Science and Its Applications, ICCSA 2019*, 166–171. doi:10.1109/ICCSA.2019.00017

Pourmousa, N., Ebrahimi, S. M., Malekzadeh, M., & Gordillo, F. (2021). Using a novel optimization algorithm for parameter extraction of photovoltaic cells and modules. *The European Physical Journal Plus*, *136*(4), 470. doi:10.1140/epjp/s13360-021-01462-4

Qais, M. H., Hasanien, H. M., & Alghuwainem, S. (2020). Parameters extraction of three-diode photovoltaic model using computation and Harris Hawks optimization. *Energy*, *195*, 117040. doi:10.1016/j.energy.2020.117040

Tong, N. T., & Pora, W. (2016). A parameter extraction technique exploiting intrinsic properties of solar cells. *Applied Energy*, *176*, 104–115. doi:10.1016/j.apenergy.2016.05.064

Villalva, M. G., Gazoli, J. R., & Filho, E. R. (2009). Comprehensive Approach to Modeling and Simulation of Photovoltaic Arrays. *IEEE Transactions on Power Electronics*, *24*(5), 1198–1208. doi:10.1109/TPEL.2009.2013862

Waly, H. M., Azazi, H. Z., Osheba, D. S. M., & El-Sabbe, A. E. (2019). Parameters extraction of photovoltaic sources based on experimental data. *IET Renewable Power Generation*, *13*(9), 1466–1473. doi:10.1049/iet-rpg.2018.5418

Ye, M., Wang, X., & Xu, Y. (2009). Parameter extraction of solar cells using particle swarm optimization. *Journal of Applied Physics*, *105*(9), 094502. doi:10.1063/1.3122082

Yegnanarayana, B. (1994). Artificial neural networks for pattern recognition. *Sadhana*, *19*(2), 189–238. doi:10.1007/BF02811896